◆ Human Brain Mapping 38:4882–4897 (2017) ◆

Pivotal Role of hMT+ in Long-Range Disambiguation of Interhemispheric Bistable Surface Motion

João Valente Duarte, Gabriel Nascimento Costa, Ricardo Martins, and Miguel Castelo-Branco*

CiBIT, ICNAS, Institute for Biomedical Imaging in Life Sciences (IBILI) - Faculty of Medicine, University of Coimbra, Portugal

Abstract: It remains an open question whether *long-range* disambiguation of ambiguous surface motion can be achieved in early visual cortex or instead in higher level regions, which concerns object/surface segmentation/integration mechanisms. We used a bistable moving stimulus that can be perceived as a pattern comprehending both visual hemi-fields moving coherently downward or as two widely segregated nonoverlapping component objects (in each visual hemi-field) moving separately inward. This paradigm requires long-range integration across the vertical meridian leading to interhemispheric binding. Our fMRI study ($n = 30$) revealed a close relation between activity in hMT+ and perceptual switches involving interhemispheric segregation/integration of motion signals, crucially under nonlocal conditions where components do not overlap and belong to distinct hemispheres. Higher signal changes were found in hMT+ in response to spatially segregated component (incoherent) percepts than to pattern (coherent) percepts. This did not occur in early visual cortex, unlike apparent motion, which does not entail surface segmentation. We also identified a role for top–down mechanisms in state transitions. Deconvolution analysis of switch-related changes revealed prefrontal, insula, and cingulate areas, with the right superior parietal lobule (SPL) being particularly involved. We observed that directed influences could emerge either from left or right hMT+ during bistable motion integration/segregation. SPL also exhibited significant directed functional connectivity with hMT+, during perceptual state maintenance (Granger causality analysis). Our results suggest that long-range interhemispheric binding of ambiguous motion representations mainly reflect bottom–up processes from hMT+ during perceptual state maintenance. In contrast, state transitions maybe influenced by high-level regions such as the SPL. *Hum Brain Mapp 38:4882–4897, 2017.*

Key words: visual motion; interhemispheric integration; decision-making; fMRI; connectivity

Additional Supporting Information may be found in the online version of this article.

Contract grant sponsor: "Projecto Operacional Regional do Centro"–BIGDATIMAGE; Contract grant numbers: CENTRO-01-0145-FEDER-000016 and MEDPersyst POCI-01-0145-FEDER-016428; Contract grant sponsor: FCT; Contract grant number: UID/NEU/04539/2013; Contract grant sponsor: COMPETE; Contract grant number: POCI-01-0145-FEDER-007440; Contract grant sponsor: Bial Foundation Fellowships; Contract grant numbers: 132/133, 373/2014, and G-02384; Contract grant sponsor: Portuguese Foundation for Science and Technology (FCT); Contract grant number: FCT-SFRH/BD/69735/2010

*Correspondence to: Miguel Castelo-Branco; Azinhaga Santa Comba, Celas 3000-548, Coimbra, Portugal. E-mail: mcbranco@fmed.uc.pt

Received for publication 5 February 2017; Revised 12 June 2017; Accepted 14 June 2017.

DOI: 10.1002/hbm.23701

Published online 28 June 2017 in Wiley Online Library (wileyonlinelibrary.com).

INTRODUCTION

Perceptual interpretation of multiple motion signals that can be combined in different ways poses processing challenges which may manifest at several levels of the visual system. These include simple computations such as motion trajectory (as in apparent motion) or more complex object/surface segmentation *versus* integration based on motion signals. This binding problem is well instantiated by the question of whether motion signals coming from co-existing contours arise from single or multiple objects. Binding of motion signals into surfaces or objects does follow simple Gestalt rules such as contour grouping and common fate. It can be studied using conditions entailing multistable perceptual states, such as plaid stimuli, created by superimposing two gratings independently moving with different orientations [Adelson and Movshon, 1982; Alais et al., 1997]. These stimuli can be used to address the question of how the visual system integrates global patterns of motion from its components.

Traditionally, there is evidence for two motion detection subsystems, a short-range system responsible for the detection of local energy spatio-temporal continuities over small displacements and a long-range system that is sensitive to higher order attributes [Albright and Stoner, 1995]. The latter may play an important role in integration/segregation processes leading to the representation of moving surfaces [Braddick, 1997; Freeman and Driver, 2008]. It is accepted that the propagation of low-level component motion responses, coding local features of the plaid, to higher level motion processing domains with larger receptive fields, integrating motion signals over space, contributes to the detection of pattern motion [Castet and Zanker, 1999]. This second stage of motion computation has been found to be achieved by neurons in MT region by performing something like an intersection-of-constraints (IOC) computational mechanism [Adelson and Movshon, 1982; Alais et al., 1994; Simoncelli and Heeger, 1998]. This mechanism requires the combination of the inputs of at least two local direction selective sensors with distinct tuning properties.

The human extrastriate middle temporal complex (hMT+) is well known to be involved in motion perception [Huk et al., 2002; Kaas et al., 2010; Kolster et al., 2010; Zeki et al., 1991] and has been strongly implicated in processing of ambiguous bistable moving stimuli, such as plaids [Adelson and Movshon, 1982; Alais et al., 1997]. We have previously shown that during exposure to plaid stimuli, hMT+ underlies the perceptual integration of pattern motion or segregation of component motion signals and that the spontaneous switches between different perceptual interpretations are directly reflected in brain activity in this region [Castelo-Branco et al., 2002]. However, plaid stimuli have highly overlapped local motion contours. This implies local integration/segregation of overlapping components, based on occlusion/transparency relationships and luminance cues. This may bias the influence of local mechanisms, as postulated by "blob-tracking" models [Adelson and Bergen, 1985; Adelson and Movshon, 1982; Alais et al., 1994]. This has hindered the investigation of long-range motion integration problems which requires the combination of far apart motion signals, that is, the study of global mechanisms underlying the perceptual disambiguation of motion signals that may be spatially separated. Thus, previous bistable surface motion paradigms leave unanswered questions concerning the neural mechanisms underlying long-range perceptual integration and segregation of spatially separated surface motion.

Here we present a new paradigm that answers this fundamentally novel question, concerning perceptual long-range integration or segregation of nonsuperimposed surface motion. We take advantage of a paradigm leading to perceptual emergence of distinct and competing stimulus interpretations using a physically constant bistable stimulus with spatially distant, nonoverlapping, and widely separate 1-D components restricted to individual visual hemi-fields. This leads to surface integration having to be necessarily long-range, that is, interhemispheric. Moving surfaces can either be perceptually parsed into different objects or interhemispherically integrated into a single moving pattern. Our stimulus consists of a global 2-D pattern with angled lines meeting in the vertical midline and moving downward, if bound together as a single surface. In the absence of physical changes, after some time, the observer will perceive the lines as two separate spatially segregated objects, one in each visual hemi-field, moving horizontally inward toward each other. Indeed, one novel aspect of this study is the fact that, with this paradigm, we set to elucidate the relative role of hMT+ in interhemispheric bistability, while excluding local "blob-tracking" mechanisms based on overlapping contours leading to local integration.

For simple visual paradigms, which do not require surface or object integration, there is evidence from electrophysiological and fMRI data that both striate and extrastriate activity underlie bilateral visual path integration [Liu et al., 2009]. This is corroborated by evidence from bistable apparent motion [Liu et al., 2004; Muckli et al., 2002, 2005; Sterzer et al., 2002], mainly with the "dot quartet," which is an ambiguous version of apparent motion that leads to percepts of either horizontal (across visual hemi-fields) or vertical (within hemi-field) motion. The quartet dots feature a simpler computational problem, and were shown to evoke V1 activation on the apparent motion trace [Muckli et al., 2005]. Nevertheless, there are studies showing that activation in primary visual cortex may be mediated by feedback from hMT+ [Sterzer et al., 2006; Wibral et al., 2009]. In fact, two recent structural studies emphasized the importance of connections with hMT+ in apparent motion processing. One found that the variability in interhemispheric integration of horizontal motion of the quartet is predicted by the properties of callosal segments connecting hMT+ [Genç et al., 2011], while the other suggests that local information transmission efficiency in bilateral pulvinar nucleus (PN) influences the probability of perceiving apparent horizontal motion through bilateral PN-MT+ tracts [Shimono et al., 2012].

Nonetheless, in the case of apparent motion there is only a change in perceived direction of motion and no explicit qualitative perceptual contrast between segmentation versus integration of object/surface motion. Thus, it remains unclear how nonoverlapped components, separated across hemi-fields, are segregated or integrated within the visual hierarchy, and the respective role of early visual vs extrastriate processing. Importantly, the novelty of our study is anchored on the fact that this particular stimulus requires integration/segregation judgements of global moving surfaces that cannot be achieved within V1, which only processes local contours. We rather hypothesize that this long-range disambiguation problem might be solved by interhemispheric functional connectivity between both hMT+. Therefore, we investigated the directed functional connectivity [Friston et al., 1994, 2013; Friston, 2011; Stephan and Friston, 2010] between hMT+ and other activated brain areas during bistable motion states using Granger causality [Goebel et al., 2003; Roebroeck et al., 2005, 2011]. We have investigated what are the brain regions subserving large-scale motion integration and surface reconstruction and also what is the role of parietal and frontal regions, in particular in which concerns top–down effects. Connectivity analysis during global motion disambiguation was of great interest to unravel the functional role of early visual areas in relation to high-level decision regions in the context of maintenance of perceptual stability.

In addition to perceptual maintenance states, we also investigated the dynamics of state transitions in perceptual decision by taking advantage of this particular stimulus requiring large scale interhemispheric. Finally, to investigate the level of involvement of regions responding during perceptual decision, we performed a whole-brain correlation analysis of the signal change with the number of perceptual reversals. The rationale was that regions critically related to the number of perceived transitions, as determined by their activity modulation as a function of the number of perceptual transitions, must be directly involved in perceptual decision-making.

MATERIALS AND METHODS

Participants

We recruited 30 healthy participants (18 male; mean age ± standard deviation = 28.37 ± 5.48 years) to take part in the study. All participants had normal or corrected-to-normal vision and no history of neurological or psychiatric disease. Participants were naive as to the specific experimental question, except two co-authors of this study. All participants were right-handed, as confirmed by Edinburgh Handedness Inventory [Oldfield, 1971]. Informed written consent, in accordance to the declaration of Helsinki, was obtained for all participants. The experiments were conducted in compliance with the safety guidelines for MR research on humans.

Ambiguous and Unambiguous Stimuli

To achieve clear-cut long-range interhemispheric perceptual integration, we used a bistable stimulus first described by Hans Wallach [Wallach, 1935; Wuerger et al., 1996] that elicits perception of one coherent object or two separate objects, separated at the vertical midline. This visual paradigm requires interhemispheric integration when perceptual coherence occurs. We also constructed a control unambiguous stimulus by adding a disambiguating background texture of dots. Both ambiguous and unambiguous stimuli are represented in Figure 1. The ambiguous stimulus, a descending roof-shaped pattern when perceived as coherent, consisted of angled black lines on a white background, mirrored at the vertical midline of the visual field and moving continuously downward. After prolonged viewing under continuous motion, the physically unchanged pattern produces two possible interpretations which alternate spontaneously: a single bound pattern moving downward—coherent motion (Fig. 1A)—or two independent surfaces moving horizontally inward—incoherent motion (Fig. 1B). Stimulus' properties reproduced the stimulus as it was first described [Wallach, 1935; Wuerger et al., 1996], as follows: contrast 100%; duty cycle 6%; spatial frequency 1.2 cycle/°; orientation 45° relative to x-axis (left-side image); motion speed 2.5°/s; stimulus size 5.5° × 6° (vertical × horizontal) visual angle in degrees. A central blue cross (visual angle 0.2°) was present as a fixation target at the visual midline to avoid gaze drift. To create a fully unambiguous control stimulus, we used the exact same bistable pattern on which we added grey dots (600 dots; contrast 10%; and visual angle 0.2°) randomly distributed throughout the image on top of the lines (Fig. 1C). The dots moved at the same speed as the grating pattern. By adding dot textures to the image one can force perception to be fully unambiguous—100% inward moving dots on each half of the image induce incoherent motion and 100% downward moving dots in the whole image induce downward coherent motion.

Reports of alternative percepts were extremely rare and participants reported confidence in categorizing their perceptual experience in either coherent or incoherent percepts. Moreover, the alternative configurations could be safely categorized as incoherent motion as a separation of both halves of the image was a common feature to all and easily identifiable as such in pilots. Thus, in this study, participants were only assigned two buttons to report either coherent or incoherent percepts.

Stimulus Presentation and Apparatus

We wrote our experiments in MATLAB R2013a (The Mathworks, Inc., Natick, MA-USA), using the Psychophysics Toolbox version 3.0 extensions [Brainard, 1997; Pelli, 1997]. The stimuli were shown inside the MR scanner by means of an LCD screen (Avotec Real Eye Silent Vision 6011, Stuart, FL 34994, USA: resolution, 1920 × 1080;

refresh rate, 100 Hz) located ~156 cm away from the participant (image size in the screen was 22.62° × 17.06° visual angle). Participants viewed the screen through a mirror mounted above their eyes. Participants responded to visual stimuli using a fiber-optical MRI-compatible response box (Cedrus Lumina LP-400, LU400 PAIR, Cedrus Corporation, San Pedro, CA 90734, USA). To confirm whether participants maintained central fixation during the experimental task, individually calibrated eye tracking data (sample frequency 1000 Hz) were recorded inside the scanner using Eyelink 1000 software (SR Research, Ottawa, Ontario, Canada).

Experimental Design and Procedure

Before entering the MR scanner, participants performed a short practice block with the ambiguous stimulus to ensure they were able to spontaneously switch perception with this stimulus. Inside the scanner, the perceptual task consisted of blocks of the ambiguous moving stimulus for 1 min, during which participants were asked to report each switch in the perceived direction of motion by pressing one of two buttons, one for coherent motion and another for incoherent motion, and holding it during the stable perceptual state until the next switch. One experimental run with the ambiguous stimulus consisted of 5 of these motion blocks preceded and followed by periods of 15 s with the static image of the stimulus. Participants were instructed to maintain fixation. A schematic representation of the experimental runs with the ambiguous stimulus is presented in Figure 1D. Each participant performed two of these experimental runs with the ambiguous stimulus and were given time to rest between runs to avoid fatigue. The unambiguous perceptual task consisted of a separate run, lasting ~6 min as well. The duration of each motion block was randomly set to 4–8 s. Each motion period contained only one of the unambiguous percepts, either coherent or incoherent motion, and was followed by a period of 8–10 s with the static image of the stimulus. Participants were instructed to maintain fixation and report the perceived direction of motion as in the ambiguous task. Data of each participant were acquired in one single scanning session of fixed duration, including both ambiguous

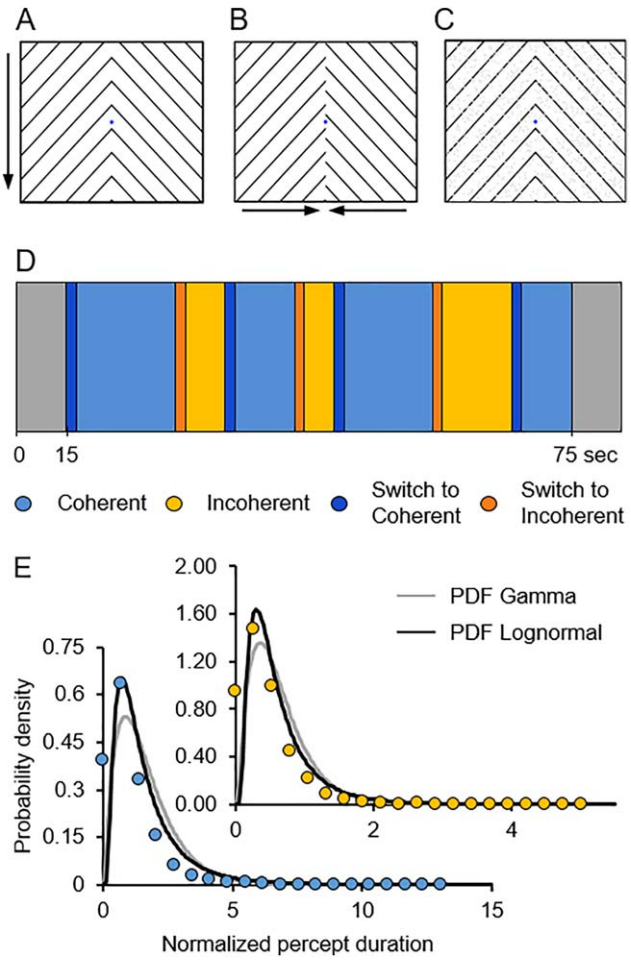

Figure 1.

(A,B) Bistability results from the continuous viewing of the ambiguous roof-shaped moving stimulus and is characterized by alternating periods of interpreting the figure in its coherent conformation (**A**), that is, both sides of the image meet at the center with no lag and are perceived as a single object moving downward, and its incoherent configuration (**B**), characterized by horizontal motion of both halves of the image as two independent objects moving towards the center, an illusory border separating both sides and lines appearing, illusorily, to be out of phase. Arrows indicate the perceived direction of motion, coherent (A) or incoherent (B). Note that the stimuli in (A) and (B) are different just for illustration purposes. (**C**) The control stimulus was an unambiguous stimulus in which we added a disambiguating background texture of grey dots. By adding the texture, we strongly induced perception of motion of the two sides of the image in the same direction as the moving dots, either coherent or incoherent. (**D**) The bistable stimulus was continuously presented in blocks of 60 s preceded and followed by 15 s of the static image of the stimulus (grey periods). Participants were instructed to report whether they perceived coherent (light blue periods) or incoherent (yellow periods) motion. The acquisition volumes in which a perceptual switch occurred were marked as events (dark blue events are switches to coherent motion; orange events are switches to incoherent motion). (**E**) Temporal dynamics of perceptual switches. Distributions of percept durations during ambiguous bistable stimulation are well described by a gamma (grey line) or lognormal distribution (black line), which are typical of a broad range of multistable phenomena. The dots are histograms of each percept's normalized duration, obtained by first normalizing percept durations per observer by dividing by the mean, and then pooling data over observers. The durations are therefore dimensionless. [Color figure can be viewed at wileyonlinelibrary.com]

and unambiguous experimental runs. Participants were given liberal time to rest between runs.

Behavioral Analysis and Perceptual Dynamics

A bistable stimulus is characterized by the fact that it allows two different perceptual interpretations. The perceptual changes are subjective experiences, with perception changing spontaneously between the different percepts and considerable interindividual differences. We conducted individual behavioral analysis of bistable perception data. We computed mean duration times for each percept and estimated the probability of a perceptual switch to occur after a particular time—the probability density function (PDF) of percept duration. Both the gamma and the lognormal distributions were fitted to the data using the maximum likelihood method to estimate the parameters, as these are two established distributions for fitting perceptual duration data of ambiguous stimuli [Borsellino et al., 1972; Brascamp et al., 2005; Zhou et al., 2004]. The goodness of fit was assessed using the Kolmogorov–Smirnov test (good fit when P value > 0.05). Results of gamma and lognormal fitting are plotted in Figure 1E.

Functional Image Acquisition

Data were collected with a Siemens Magnetom TIM Trio 3T research scanner (Siemens, Munich, Germany) with a phased array 12-channel birdcage head coil. The MR scanning session began by acquiring a 3-D anatomical T1-weighted MPRAGE (magnetization-prepared rapid gradient echo) pulse sequence (TR = 2530 ms; TE = 3.42 ms; TI = 1100 ms; flip angle 7°; 176 single-shot interleaved slices (no gap) with voxel size $1 \times 1 \times 1$ mm; FOV 256 mm). Functional images (minimum of 2 ambiguous and 1 unambiguous run) were acquired axially using a T2*-weighted gradient echo (GE) echo planar imaging (EPI) sequence covering the whole brain. Each functional series consisted of 180 volumes (TR = 2000 ms, TE = 40 ms, flip angle = 90°, 35 interleaved slices (no gap) with voxel size $3 \times 3 \times 3$ mm; FOV 256 mm) of BOLD signal measurements.

fMRI Data Preprocessing

At the beginning of each acquisition sequence, the first 2 volumes of functional data were automatically discarded in the scanner to allow the magnetization to reach a steady state. The data were analyzed using BrainVoyager QX 2.8 (Brain Innovation, Maastricht, The Netherlands). Functional volumes were realigned, corrected for interleaved slice-scanning time, and linear trends were removed from the signal. Interscan head motion correction was performed by adjusting all the functional runs with the first functional run presented right after the anatomical scan. Motion parameters were included in the statistical analysis as regressors of no interest. We also applied temporal high-pass filtering (2 cycles per run) to functional images to compensate for a slow fMRI signal drift. We then coregistered functional scans with the participants' corresponding anatomical (T1-weighted) scan and applied slight spatial smoothing (FWHM 3 mm) for individual data analysis. For group analysis, we spatially normalized both anatomical and functional data into Talairach stereotactic space and moderately spatially smoothed fMRI data (FWHM 6 mm). The cortical sheets of the individual participants and a Talairach template brain were reconstructed as described elsewhere [Kriegeskorte and Goebel, 2001; Linden et al., 1999] and used to overlay functional data and statistical results.

Individual MT+ Localization

We investigated neural responses to bistable perceptual states within hMT+ and higher order areas. The left and right hMT+ were functionally localized in every participant with an independent individual GLM analysis of the unambiguous motion experiment. The hMT+ was defined as the voxels in the middle temporal region responding significantly to the balanced contrast of motion [Coherent + Incoherent > Static]. The individual statistical maps were thresholded at P value = 0.05, FDR-corrected.

Statistical Data Analysis

The individual reports of coherent and incoherent motion were used in standard general linear model (GLM) analysis at individual and group levels (RFX-GLM, see Penny et al. [2003]), with separate predictors of transient switch-related activity (*switch* predictors) or activity during stable perceptual states between two successive switches (*state* predictors). We subtracted each individual's reaction time, computed from the unambiguous experiment, to every time of button press to more reliably identify the perceptual switches. Switch predictors had a duration of one volume (2 s), the one when they occurred. We excluded the first perceptual period of each motion block to avoid unspecific stimulus onset effects. We excluded the first volume after motion stops to avoid motion aftereffects. In the unambiguous experiment, predictors were determined from the stimulation protocol. We tested the contrast between different perceptual states with a group analysis, as our main contrast of interest. Additionally, we computed the whole-brain group-level contrast of switch-related transient activity against perceptual states. Statistical maps were corrected for multiple comparisons using the false discovery rate (FDR) method for correction of multiple comparisons at P value <0.05 at single-subject level and P value <0.001 at group level. An additional strategy, relying on a finite impulse response (FIR) model, was also used to deal with the issue of different block durations (which is in effect already taken into account by the standard GLM model). We therefore employed a GLM deconvolution analysis within regions-of-interest (ROIs) to

estimate the BOLD responses for each percept. A deconvolution analysis as implemented consists of an alternative GLM analysis that allows estimating the unmixed BOLD responses for each event type. The FIR model makes no assumption about the shape of the hemodynamic response and is useful in cases where differences in time courses may exist across conditions. This allows a more flexible fitting of the model and allows the user to compare conditions on the single data point basis (see, e.g., Glover [1999] for a detailed explanation). As the results of the standard and deconvolution GLM approaches concurred, we are confident in our conclusions about the signal modulation in response to this bistable stimulus.

Connectivity Analysis: Granger Causality Mapping

The directed influence between hMT+ and other regions of the brain was investigated using Granger Causality Mapping (GCM) in BrainVoyager QX, a technique that allows the computation of directed functional connectivity measures from fMRI data using the theory of Granger causality [Goebel et al., 2003; Roebroeck et al., 2005]. In short, GCM is computed for a given ROI, which is considered the reference region, and the result contains both sources of influence to the reference region and targets of influence from the reference region to any other voxel in the brain. We used each hMT+ in the left and right hemisphere of the brain to compute outgoing and incoming influence to these ROIs as detailed by Roebroeck et al. [2005]. We then computed RFX-GCM maps at the group level by performing one-sample t tests of connectivity measures and corrected the maps with cluster extent threshold at P value < 0.05, which estimation was based on Monte Carlo simulations (1000 iterations, primary threshold P value < 0.001 uncorrected at the single voxel level, and P value < 0.05 corrected at the cluster level). The minimum cluster size was 37 contiguous voxels.

To be able to compute GCM maps, we opted not to split protocols according to reported perceptual switches, for two reasons: (1) this would break the temporal structure of brain activity; (2) our question concerned dynamics of perceptual decision and not its particular content. We computed GCMs using the whole ambiguous bistable motion periods as a single condition, to get an estimate of connectivity between brain regions during the perceptual decision task.

Correlation Analysis to Uncover Regions Directly Involved in Perceptual Transitions

We performed a whole-brain correlation analysis of the signal change during the perceptual decision task with the number of perceptual reversals, using the same software tool. Beta values, resulting from the RFX-GLM analysis, were correlated with an external covariate (number of individually reported perceptual switches) during ambiguous stimulation periods. The resulting whole-brain maps containing r values were corrected for multiple comparisons using a cluster extent threshold at P value < 0.05 and voxel extent, which estimation was based on Monte Carlo simulations (1000 iterations, primary threshold P value < 0.001 uncorrected at the single voxel level, and P value < 0.05 corrected at the cluster level). Significant clusters include at least 24 contiguous voxels.

RESULTS

Behavioral Analysis

During bistable ambiguous stimulation participants perceived on average the coherent condition for 6.71 ± 0.38 s (mean $\pm$ SEM) while the mean duration of the incoherent condition was 2.60 ± 0.21 s. The mean duration of the coherent percept was significantly longer than that of incoherent (P value < 0.001, Wilcoxon signed rank test) (see Methods section for analyses controlling for distinct durations). Similar to other bistable stimuli, the durations of each percept followed a gamma or lognormal distribution (Fig. 1E), which are typical of perceptual rivalry [Leopold and Logothetis, 1999; Zhou et al., 2004]. Overall, only 2 out of 30 participants failed to achieve a significant gamma or lognormal fit for both coherent and incoherent duration. This might be ascribed to a lower number of data points in individual data sets for these subjects, and not to a significant difference in perception of the illusion. In fact, these subjects followed a similar behavior as the group average, with longer coherent percepts than incoherent. For this reason, they were not excluded from the analysis.

On the other hand, during the control unambiguous experiment observers were very accurate to confidently report the perceived direction of motion as matching the direction of the dotted texture, either coherent or incoherent.

Fixation data

We monitored fixation by visual inspection during all experiments. The analysis of fixations was performed on the data of 23 participants just as a quality control of the experiment. Data from seven participants were not recorded due to eye-tracker malfunction within the scanner. Averages of fixation time were calculated based on the recorded gaze behavior with Eyelink Data Viewer, version 1.11.900. A fixation duration threshold of 150 ms was used and 87% of participants had good-quality eye tracking data recorded, with a minimum of 75% of the time fixating. A rectangular area of interest ($2.5° \times 3°$) was defined on the center of the image, within which the global average of successful fixation for those participants was 90% (SD = 5.32) and 89% (SD = 5.13) for ambiguous and unambiguous stimuli, respectively.

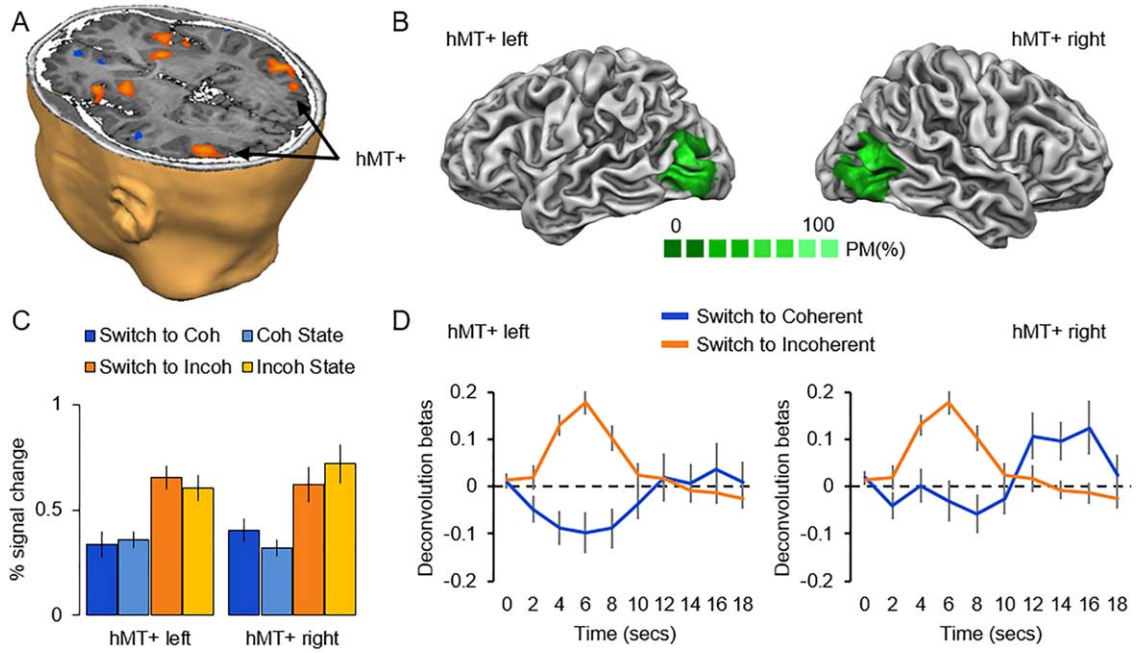

Figure 2.

(**A**) Group analysis of perceptual contrast [incoherent > coherent] shown in a template brain in Talairach space. RFX-GLM statistical map revealed only a few selective significant clusters (*P* value corrected for FDR at 0.001 level) in motion selective region hMT+ and decision areas as the insula and putamen. (**B**) Probability maps of left and right hMT+ regions individually defined in all 30 participants from the unambiguous experiment. The maps are superimposed on a template reconstruction of the cortex in Talairach space. (**C**) To avoid circularity in analysis, individually defined hMT+ regions shown in (B) were used to apply individual ROI-GLM analysis and extract activity in response to perceptual switches and perceptual stable states of coherent motion of one surface and incoherent motion of two distinct surfaces in the ambiguous task. The bar plot represents average group data. Note that there was not a significant difference in response to perceptual switches compared to the response to the perceptual state of the same percept, coherent, or incoherent motion (see Table I with one-way repeated measures ANOVA and post hoc pairwise comparisons). Nonetheless, average activity is higher when two stable moving surfaces are perceived than one single surface is interhemispherically integrated. (**D**) To extract unmixed responses to switch events, we applied deconvolution analysis within individually defined hMT+. Deconvolution plots clearly show a differential response of hMT+ to the perceptually distinct switch types. Error bars in (**C**) and (**D**) represent ±SEM. [Color figure can be viewed at wileyonlinelibrary.com]

GLM Analysis of Bistable Motion

The GLM group analysis of contrast differences between episodes with differing percepts revealed regions with higher activity during perception of incoherent motion of two surfaces than during long-range coherent perception of one surface spanning both hemi-fields. Figure 2A shows the clusters with the highest contrast (FDR corrected P value < 0.001) in Talairach space. Specific clusters were identified as corresponding to the hMT+ of both hemispheres, and also the bilateral insula and bilateral putamen. It is worth pointing out the absence of early visual cortical activation by this perceptual contrast.

Single-subject analysis in hMT+

To investigate modulation of activity within hMT+ and to prevent circularity in the analysis, we individually defined hMT+ from the unambiguous experiment. The probability maps of location of hMT+ are shown in Figure 2B. The average size of hMT+ was 1457 voxels on the left (Talairach coordinates $X = -45 \pm 3$; $Y = -69 \pm 5$; $Z = 5 \pm 6$) and 1451 voxels on the right (Talairach coordinates $X = 46 \pm 3$; $Y = -65 \pm 5$; $Z = 4 \pm 6$).

We then extracted mean activity within hMT+ ROIs with standard GLM (Fig. 2C) and deconvolution plots (Fig. 2D) of response to perceptual switches and perceptual stable states.

From standard GLM, we can clearly see the modulation of activity depending on whether participants integrate 1-D direction of motion information from both hemispheres and perceive one 2-D coherent surface or perceive instead two incoherent surfaces. Average group data (Fig. 2C and Table I) confirmed that perception of long-range pattern motion resulted, on average, in significantly lower activity

TABLE I. One-way repeated measures ANOVA of BOLD activity within left and right hMT+ in response to perceptual switches and perceptual states during bistable motion

		L hMT+	R hMT+
Main effect of perception *(switches* and *states)*	df (error)	1.966 (87)	2.230 (87)
	F	12.571	8.245
	P value	<0.001	<0.001
	η_P^2	0.302	0.221
Switch to coherent vs coherent state	P values	1.000	0.692
Switch to coherent vs switch to incoherent		0.008	0.292
Switch to coherent vs incoherent state		0.009	0.002
Coherent state vs switch to incoherent		<0.001	0.016
Coherent state vs incoherent state		<0.001	0.002
Switch to incoherent vs incoherent state		1.000	1.000

η_P^2 = partial eta squared, a measure of the estimated effect size; df = degrees of freedom. Pairwise comparisons were corrected with Bonferroni correction for multiple comparisons. When sphericity was not verified, we used a Greenhouse–Geisser correction.

than component motion, which was further demonstrated by the RFX analysis. The response to component motion (incoherent) was significantly higher than the response to pattern motion (coherent) in both ambiguous and unambiguous experiments (Supporting Information, Fig. 1 and Table I). The analysis of specific transient (phasic) response to perceptual switches revealed that it is not significantly different from the tonic response to subsequent corresponding perceptual states within hMT+ (Fig. 2C) as confirmed by a repeated measures ANOVA (Table I).

We employed a deconvolution analysis to investigate the time course of transient responses to perceptual switch events (Fig. 2D). Note that the graphs have to be interpreted in terms of relative activity levels: as one condition is the baseline for the other condition, hence a negative time course does not necessarily mean diminished brain activity during that condition, rather corresponding to a smaller increase in brain activity relative to true baseline (no stimulation). Interestingly, we could again observe a higher response to perceptual switches to component/incoherent motion than to pattern/coherent motion, suggesting that hMT+ is more recruited in the transitions that do not result in integration but instead in segmentation. At the group level, we observed that signal changes in response to the switch to component/incoherent motion were significantly higher than the response to the switch to pattern/coherent motion both in left (P value = 0.0014, paired t test) and right hMT+ (P value = 0.0486, paired t test).

Whole-brain group analysis

The whole-brain RFX-GLM group analysis of contrast differences between ambiguous bistable percepts of motion, either coherent or incoherent, and the static stimulus (i.e., motion responses regardless of the percept) revealed regions with significant changes in motion selective regions, and parietal and frontal decision areas, which are shown in Supporting Information, Figures 2 and 3. The coordinates of each cluster's peak voxel in Talairach space are presented in Supporting Information, Table II. Notably, only visual regions hMT+ and also V3/V3A in both hemispheres, and superior parietal lobule, show a clear difference in response amplitude between coherent and incoherent percepts in both ambiguous and unambiguous experiments, corroborating the analysis depicted in Figure 2A.

Regarding perceptual state transitions, the statistical map of the whole-brain RFX-GLM analysis of switch-related transient activity is presented in Figure 3. In Table II, we show Talairach coordinates, t value and number of voxels of each cluster showing a significant contrast of perceptual switch-related activity compared to perceptual state-related activity.

We found significant responses in decision and executive function related cortical areas, such as the insula, prefrontal cortex, dorsal anterior cingulate, and inferior frontal gyrus. Notably, the cluster with the highest significant signal change was found in the left superior parietal lobule, a region known for its involvement in perceptual transitions [Intaitė et al., 2016; Zaretskaya et al., 2010]. In Supporting Information, Figures 4 and 5, we present the group results of RFX-GLM as plots of beta values for each condition. Additionally, for each significant cluster identified, we also show the time courses of response to both perceptual switches and perceptual states, as extracted from deconvolution analysis. Interestingly, we also found highly significant switch-related signal changes bilaterally in the cerebellum and in particular the left thalamus, in response to perceptual switches.

Granger Causality Analysis

The directed influences to and from hMT+ in both hemispheres was investigated using the concept of Granger causality [Goebel et al., 2003; Roebroeck et al., 2005, 2011].

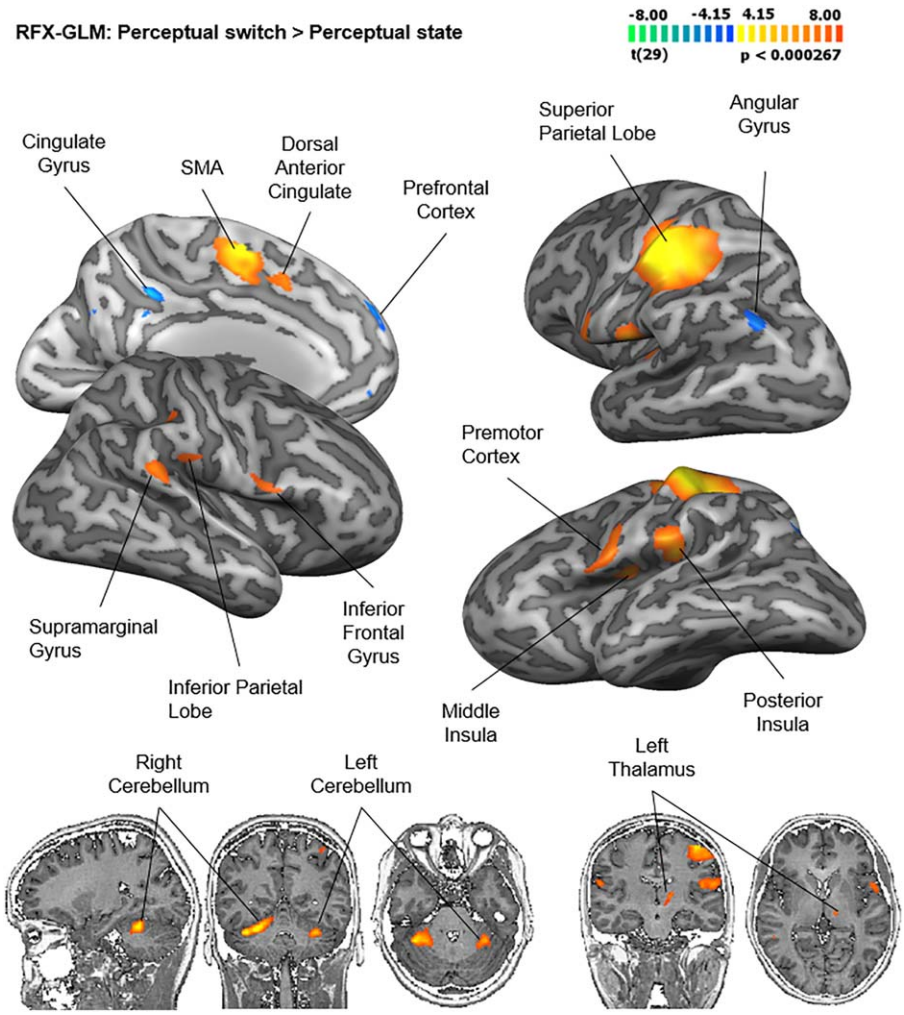

Figure 3.

Signal changes during ambiguous bistable motion with a GLM approach to investigate differences in switch-related transient response compared to stable perceptual states. Group analysis shown in a template inflated brain in Talairach space. RFX-GLM contrast analysis of switch-related activity revealed significant clusters (*P* value corrected for FDR at 0.001 level) in motor, premotor, and decision areas. We also observed significant clusters in the cerebellum and left thalamus. SMA, supplementary motor area. [Color figure can be viewed at wileyonlinelibrary.com]

This method and several variants have been applied to neurophysiological data to gain insight in the direction of influences between neural systems [Seth et al., 2015]. We computed whole-brain group RFX-GCM maps showing voxels that are influenced by the activity in left or right hMT+, individually defined at the single-subject level. The results are presented in Figure 4. Granger causality maps revealed significant directed influences during ambiguous bistable motion from the individually defined left hMT+ to left prefrontal cortex (BA10), left middle temporal gyrus (BA21), early visual cortex in the left hemisphere, and surrounding areas in hMT+ including the kinetic occipital (KO) region [Dupont et al., 1997; Van Oostende et al., 1997]. There was also significant connectivity from left hMT+ to the contralateral hemisphere, namely, the right V3/V3A region, right hMT+ complex, a more posterior region than hMT+ corresponding to the right KO area, and dorsal right superior parietal lobule (BA7).

Interestingly, the analysis of connectivity with right hMT+ as reference region showed significant influence also to right BA7 but in the region of the precuneus, which plays a role in integration of visual and motor information, and right V3/V3A. Additionally we observed significant connectivity with ipsilateral areas in middle temporal gyrus (BA21), hMT+ complex, KO area and early visual cortex as with the left hMT+. Notably, hMT+ in both

TABLE II. Summary of RFX-GLM results revealing clusters with significant (*P* value corrected for FDR at 0.01 level) perceptual switch-related transient responses

Region	Peak coordinates (Talairach)			*t*(29)	Number of voxels
	X	*Y*	*Z*		
L Superior parietal lobule (SPL)	−45	−28	52	10.06	10,510
R Cerebellum	27	−46	−23	9.56	3,652
Supplementary motor area (SMA)	−6	−3	52	8.46	2,250
L Cerebellum (Culmen)	−30	−46	−26	7.23	746
L Middle insula (BA13)	−42	−7	16	7.23	726
L Posterior insula	−48	−22	16	7.15	1,986
L Thalamus	−15	−19	10	6.41	263
R Superior parietal lobule (SPL)	51	−25	28	6.04	544
L Premotor cortex (BA 6)	−57	2	13	5.84	1,313
Dorsal anterior cingulate (BA32)	−6	11	37	5.82	498
R Supramarginal gyrus	54	−34	22	5.79	831
R Inferior frontal gyrus (IFG)	54	2	19	5.17	332
R Inferior parietal lobule (IPL)	48	−34	46	4.78	392
Cingulate gyrus (BA 31)	−6	−37	34	−7.23	658
L Prefrontal cortex (BA9/10)	−3	47	31	−6.02	813
L Precuneus/angular gyrus (BA39)	−39	−67	37	−5.84	1,290
R Posterior insula	−9	65	19	−5.74	342

R, right; L, left. The number of voxels is based on the resolution of the anatomical dataset $1 \times 1 \times 1$ mm^3.

hemispheres showed significant directed functional connectivity with each other during bistable motion presentation. The hMT+, however, never showed incoming directed connectivity from higher level regions, and was therefore the (bottom–up) causal source of influence.

Correlation Analysis Reveals Brain Regions That Modulate Their Activity as a Function of the Number of Perceptual Transitions

We performed a whole-brain correlation analysis between brain activity patterns and the individually reported perceptual switches. This provides an additional way of identifying brain regions critically related to perceptual decision-making (switches). The correlation between the contrast *ambiguous motion versus static* and the individual perceptual reversal rates showed strong positive correlations in the right anterior insula (BA 13; Talairach coordinates: $X = 44$, $Y = 1$, $Z = -1$) and left primary motor cortex (BA 4, Talairach coordinates: $X = -27$, $Y = -27$, $Z = 50$) ($r > 0.55$ with $P < 0.03$, corrected). A negative correlation was found in the right dorsolateral prefrontal cortex (BA 9, Talairach coordinates: $X = 35$, $Y = 35$, $Z = 30$). See Figure 5 with the *r* map.

DISCUSSION

In this study, we investigated the neural correlates of perceptual decision-making requiring long-range integration *versus* segregation of surface motion. Accordingly, visual information had to be integrated or segregated across hemispheres under nonlocal conditions in which components do not overlap, which is a crucial aspect of the current paradigm. We observed a close relation between activity in hMT+ and perceptual switches of bistable motion bound or unbound across visual hemifields. The occurrence of perceptual switches was, as expected, unpredictable but perceptual dynamics followed typical gamma or lognormal distributions [Borsellino et al., 1972; Kaneoke et al., 2009; Kline et al., 2004; Leopold et al., 2002; McDermott et al., 2001; Sterzer et al., 2002], denoting the presence of competing neural representations [Brascamp et al., 2005; Leopold and Logothetis, 1999; Zhou et al., 2004].

Our psychophysical and imaging data are consistent with the notion of two stages in the processing of motion information. We hypothesize that processing at the first level occurs mainly through component neurons (responding to small segments of the lines) but also pattern neurons, responding to each half-image as a global object [Albright and Stoner, 1995; Movshon and Newsome, 1996]. If outputs of this first stage are not integrated into the next stage, processing would lead to the perception of the two surfaces moving incoherently inward. The second stage seems to rely on a smaller population of pattern neurons that bind all motion signals into the percept of a single 2-D surface. Our fMRI data is in accordance with this hypothesis, as higher signal changes were found in hMT+ in response to incoherent percepts than to coherent percepts. This was observed at the single-subject level (Fig. 2), further suggesting that hMT+ itself is directly involved in the disambiguation mechanism of ambiguous and spatially separate motion representations, possibly through

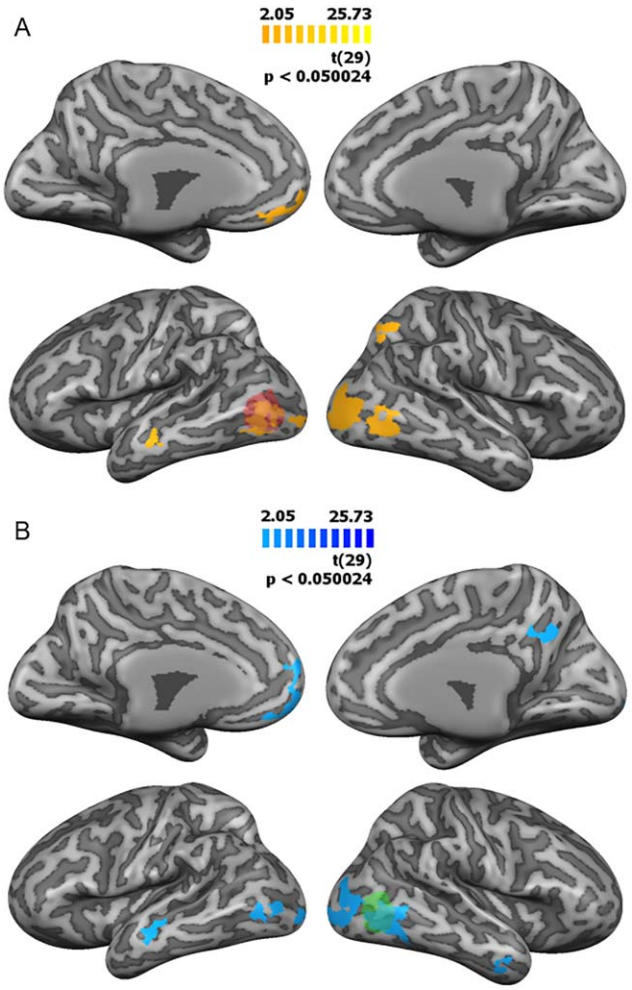

Figure 4.

RFX Granger causality mapping with the (**A**) left hMT+ and (**B**) right hMT+ individually defined in each participant as reference regions (probability maps of individual hMT+ in the left and right hemispheres are shown in shaded red and green, respectively). The highlighted regions showed a significant directed (bottom-up) influence from left and right hMT+ in orange and blue, respectively (statistical maps of *t* test GCM > 0 corrected with cluster extent threshold at *P* value < 0.05, minimum cluster size of 37 voxels). [Color figure can be viewed at wileyonlinelibrary.com]

competitive reconfiguration of neural populations [Castelo-Branco et al., 2002; Huk and Heeger, 2002; Serences and Boynton, 2007].

Importantly, we present for the first time neuroimaging evidence of interhemispheric long-range perceptual 2-D integration or 1-D segregation of locally nonoverlapping moving surfaces in hMT+ but not in the early visual cortex (in a broad sense, given that no retinotopic mapping was performed). This suggests that to solve such a global integration *versus* segregation problem a local low-level monocular mechanism such as the "blob tracking" model is not sufficient [Adelson and Bergen, 1985; Adelson and Movshon, 1982; Alais et al., 1994], hence representing a higher level computational problem. On the one hand, this goes beyond bistable apparent motion paradigms (studied mainly with the "motion quartet") in which activity related to the path of motion was found as early as in V1 but do not entail surface segmentation *versus* integration conflict [Liu et al., 2004; Muckli et al., 2002, 2005; Rose and Büchel, 2005; Sterzer et al., 2002]. On the other hand, this novel long-range paradigm extends previous work with disambiguation of local plaid motion [Adelson and Movshon, 1982; Burke et al., 1994; Castelo-Branco et al., 2000, 2002, 2009; Kozak and Castelo-Branco, 2009; Wenderoth et al., 1994], as component surfaces were critically nonoverlapping and required long-range integration. There is previous evidence from animal studies that neurons in V1 may be able to represent and encode pattern motion signals [Guo et al., 2007; Schmidt et al., 2006], although the responses of neurons to such motion may not be purely pattern-selective [Tinsley et al., 2003]. Such neurons are likely to be part of the first stage of motion analysis, as projections to hMT+ mostly carry one-dimensional component motion information, generating signals to be combined by MT pattern neurons by performing something like an intersection-of-constraints (IOC) computation [Adelson and Movshon, 1982; Alais et al., 1994; Simoncelli and Heeger, 1998]. A recent human fMRI study also suggested the involvement of V1 in plaid motion processing [van Kemenade et al., 2014]. Nonetheless, our findings with this nonoverlapping stimulus are consistent with the explanation of the coding of 2-D motion in hMT+ by the IOC model (which implies the combination of motion inputs with distinct directional tuning) and suggest that this is the case even when components are widely separate across hemi-fields, supporting the role of hMT+ in perceptual disambiguation of long-range bistable surface motion. In spite of the fact that we did not find evidence for the involvement of V1, some of the surround suppression in V1 is dependent on feedback from MT, which is thought to be useful for resolving conflicting local motion signals [Pack et al., 2003].

To specifically analyze transient signal changes related to perceptual switches, we performed report-informed deconvolution and ROI-GLM analyses within hMT+. We observed that switch-related activity was higher for perceptual transitions to incoherent/component than to coherent/pattern motion (Fig. 2 and Table I), as were also in the subsequent perceptually stable periods. This further confirms the differential activation of hMT+ in perceptual disambiguation of long-range integration/segregation of motion.

Whole-brain analysis on the switch-related events revealed prefrontal, insula, and cingulate areas (Fig. 3), suggesting that these regions and hMT+ can trigger perceptual switches, in spite of the fact that the latter

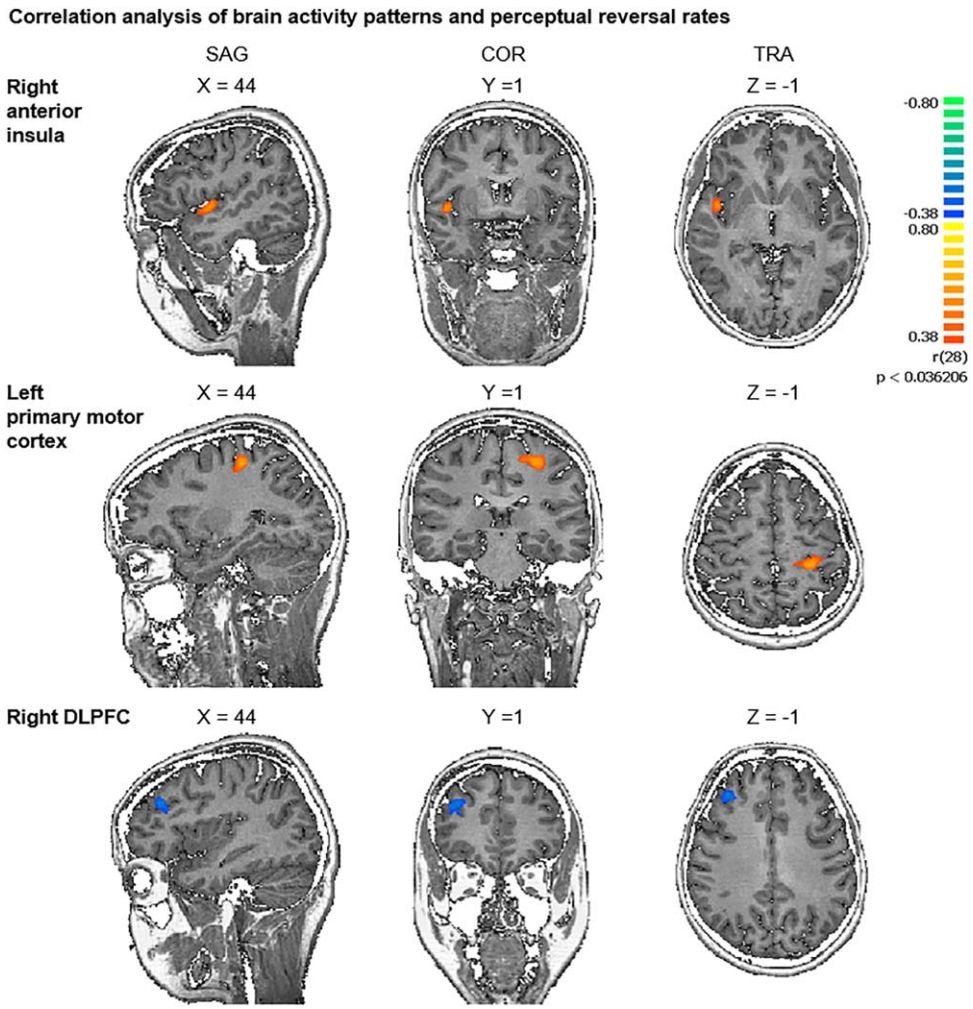

Figure 5.

Correlation analysis of brain activity patterns and perceptual reversal scores. The correlation map was calculated by contrasting ambiguous motion periods versus static periods and correlating this with the individual perceptual reversal rates. The correlation of contrast and perceptual switches was performed in a whole-brain analysis ($r > 0.55$ with P value < 0.05, cluster-level corrected with minimum cluster size of 24 voxels). The images are in radiological convention. DLPFC, dorsolateral prefrontal cortex; SAG, sagittal; COR, coronal; TRA, transaxial. [Color figure can be viewed at wileyonlinelibrary.com]

dominates during the perceptual state maintenance, as revealed by GCM analysis. This adds to the notion that bistable perception has both bottom–up and top–down influences in perceptual decision-making [Kleinschmidt et al., 1998; Knapen et al., 2011; Leopold and Logothetis, 1999; Long and Toppino, 2004; Naghavi and Nyberg, 2005; Weilnhammer et al., 2013; Wernery, 2013].

Notably, we found a large and highly significant cluster in the superior parietal lobule (SPL) related to perceptual decisions, which seems to be part of the decision network involving hMT+, either in terms of switch-related or state-related activity. The enhanced BOLD responses in SPL in response to perceptual decisions has been previously reported in fMRI studies [Knapen et al., 2011; Lumer et al., 1998; Lumer and Rees, 1999; Reddy et al., 2011; Weilnhammer et al., 2013]. Our results seem to agree with recent studies which revealed that switch-related fronto-parietal BOLD activity can be found in relation to perceptual switches irrespective of the role of other brain regions involved in behavioral choice [Brascamp et al., 2015; Intaitė et al., 2016]. Furthermore, TMS studies [Carmel et al., 2010; Kanai et al., 2010, 2011; Zaretskaya et al., 2010] suggest a causal role for SPL in generating perceptual decisions, with a right-hemispheric bias. Remarkably, we found significant directed functional connectivity of left hMT+ with dorsal right SPL. This finding adds to recent

observations that perceptual switches may be triggered by changes in connectivity between lower visual areas and parietal cortex [Megumi et al., 2015].

In fact, connectivity analysis yielded important insights into the maintenance of perceptual states for this specific interhemispheric stimulus, which might mainly induce bottom-up processes driven by hMT+, in agreement with recent evidence of strong feedforward intrinsic connectivity from lower-level feature-specific regions to dorsolateral prefrontal cortex (DLPFC) during perceptual decision-making [Lamichhane and Dhamala, 2015]. We found also directed influences from hMT+ to lower level visual areas V3/V3A, predominantly in the right hemisphere, which agrees with reports that activation in V3A underlies motion coherence [Aspell et al., 2005; Castelo-Branco et al., 2002; Tootell et al., 1997] and decoding between coherent and incoherent contexts, possibly through higher extrastriate cortex feedback [Schwarzkopf et al., 2011]. Interestingly, we found directed influences from left and right hMT+ to the contralateral hMT+ (homotopic), suggesting interhemispheric alternation of directed influences. Our results seem to be reminiscent of data suggesting stronger oscillatory coupling between right and left visual cortices during perception of horizontal motion compared with vertical motion, with apparent motion stimuli [Rose and Büchel, 2005]. A very recent study suggested coupling of activity between visual homologous areas during resting state and the same apparent motion task, although the authors did not test association with perceptual discrimination between horizontal (interhemispheric) or vertical motion [Genç et al., 2016]. Our connectivity analysis was carried out using a model-free approach to investigate directed functional connectivity, which measures the directed influence one brain region exerts over another [Friston et al., 1994, 2013; Friston, 2011; Stephan and Friston, 2010]. Although this method and several variants have been applied to neurophysiological data to gain insight in the direction of influences between neural systems [Seth et al., 2015], the use of Granger causality for mapping causal inferences from fMRI data is strongly debated as it presents potential limitations such as the variability of the hemodynamic response across regions (and participants), in particular when accompanied by down sampling and/or measurement noise, may lead to incorrect inferences [Friston et al., 2013; Seth et al., 2013].

Moreover, we cannot exclude that state transitions may be modulated by top-down mechanisms originated in higher level regions such as mid-frontal regions and the insula, which showed significant switch-related activity and correlated with perceptual decision both in our study and others [Rebola et al., 2012; Stottinger et al., 2015]. Interestingly, we found a positive correlation between brain activity patterns and the number of individually reported perceptual switches in the right anterior insula (BA 13). Recently, Lamichhane et al. [2016] observed that significantly higher BOLD response in the insula was associated with the ambiguity of sensory information in different perceptual tasks and decision-making difficulty. In our study, the response in the right anterior insula also increased in the context of more ambiguity (higher number of reversals), irrespective of difficulty (as our task did not involve difficult sensory or perceptual discriminations). Notably, a negative correlation (decreased activity with more reversals) was found in the right DLPFC (BA 9, but not BA46). This is as well in accordance with a previous study [Knapen et al., 2011], and illuminates the debate on the different role of distinct frontal areas in perceptual decision. There are neuroimaging studies suggesting that frontal regions participate in initiating spontaneous switches in ambiguous perception [Sterzer and Kleinschmidt, 2007]. TMS of frontal areas affects voluntary top–-down modulation of perceptual switches, but not necessarily by triggering transitions [de Graaf et al., 2011]. When observers passively experienced rivalry without reporting perceptual alternations differential neural activity in frontal areas was absent [Frässle et al., 2014]. Although in paradigms using ambiguous stimuli the rationale is to isolate effects of perceptual changes that do not reflect changes in the sensory input, there is emerging evidence that active report may confound the neural correlates of bistable perception with various cognitive components, such as attention, working memory or expectation, which might compromise inferences regarding the role of frontal and/or parietal regions [Intaitė et al., 2014, 2016; Kleinschmidt et al., 1998; O'Craven et al., 1997]. As recently reviewed, participants' perceptual contents can be reliably inferred from physiological measures, such as eye movements or pupil size [Tsuchiya et al., 2015]. Combining the possibility to remove stimulus-related confounds (with ambiguous stimuli) with this kind of no-report paradigms to search for the true neural correlates of bistable perception may help to dissect the role of top–down modulation effects of perceptual decision-making, namely, during state transitions and perceptual state maintenance in hMT+. Nonetheless, our data provide evidence on the putative site of perceptual grouping operations underlying the decision between long-range fusion and segregation of moving surface objects. Future studies should elucidate the role at different time scales of bottom–up *versus* top–-down mechanisms in perceptual decision, and in particular, the role of interactions within hMT+ *versus* external sources of influence triggering perceptual transitions of physically constant true surface motion.

CONCLUSION

In this study, we found an important role for hMT+ in long-range integration of global interhemispheric surface motion from spatially segregated (across hemispheres) 1-D components. These findings add to previous ones concerning local motion integration, and are in contrast with other paradigms which show significant involvement already at the level of primary visual cortex, such as apparent

motion. We found evidence of higher signal changes in hMT+ in response to incoherent percepts, which is consistent with the two stage model of motion processing (with a much larger neural population responding to component motion at both stages during incoherent perception).

We found evidence that long-range interhemispheric binding of ambiguous motion representations seems to reflect bottom–up processes within hMT+ during perceptual state maintenance. In contrast, state transitions may be influenced by top–down mechanisms originated in high-level regions such as the SPL.

In sum, using a novel paradigm with a physically constant stimulus requiring long-range perceptual integration across hemispheres, we found a critical role for hMT+/V5 in bottom–up tonic perceptual state maintenance, while higher level regions contributed to phasic switches. This novel view provides additional insights into the circuitry underlying long-range interactions during perceptual decision making in the visual system.

ACKNOWLEDGMENTS

We thank Carlos Ferreira, João Marques and Sónia Afonso from ICNAS, University of Coimbra, for their help with MRI procedures.

CONFLICT OF INTEREST

The authors declare no competing financial interests.

REFERENCES

Adelson EH, Bergen JR (1985): Spatiotemporal energy models for the perception of motion. J Opt Soc Am A 2:284–299.

Adelson EH, Movshon JA (1982): Phenomenal coherence of moving visual patterns. Nature 300:523–525.

Alais D, Wenderoth P, Burke D (1994): The contribution of one-dimensional motion mechanisms to the perceived direction of drifting plaids and their aftereffects. Vision Res 34:1823–1834.

Alais D, Wenderoth P, Burke D (1997): The size and number of plaid blobs mediate the misperception of Type-II plaid direction. Vision Res 37:143–150.

Albright TD, Stoner GR (1995): Visual motion perception. Proc Natl Acad Sci USA 92:2433–2440.

Aspell J, Tanskanen T, Hurlbert A (2005): Neuromagnetic correlates of visual motion coherence. Eur J Neurosci 22:2937–2945.

Borsellino A, De Marco A, Allazetta A, Rinesi S, Bartolini B (1972): Reversal time distribution in the perception of visual ambiguous stimuli. Kybernetik 10:139–144.

Braddick O (1997): Local and global representations of velocity: Transparency, opponency, and global direction perception. Perception 26:995–1010.

Brainard DH (1997): The psychophysics toolbox. Spat Vis 10: 433–436.

Brascamp J, Blake R, Knapen T (2015): Negligible fronto-parietal BOLD activity accompanying unreportable switches in bistable perception. Nat Neurosci

Brascamp JW, van Ee R, Pestman WR, van den Berg AV (2005): Distributions of alternation rates in various forms of bistable perception. J Vis 5:287–298.

Burke D, Alais D, Wenderoth P (1994): A Role for a low level mechanism in determining plaid coherence. Vision Res 34: 3189–3196.

Carmel D, Walsh V, Lavie N, Rees G (2010): Right parietal TMS shortens dominance durations in binocular rivalry. Curr Biol 20:799–800.

Castelo-Branco M, Formisano E, Backes W, Zanella F, Neuenschwander S, Singer W, Goebel R (2002): Activity patterns in human motion-sensitive areas depend on the interpretation of global motion. Proc Natl Acad Sci 99:13914–13919.

Castelo-Branco M, Goebel R, Neuenschwander S, Singer W (2000): Neural synchrony correlates with surface segregation rules. Nature 405:685–689.

Castelo-Branco M, Kozak LR, Formisano E, Teixeira J, Xavier J, Goebel R (2009): Type of featural attention differentially modulates hMT+ responses to illusory motion aftereffects. J Neurophysiol 102:3016–3025.

Castet E, Zanker J (1999): Long-range interactions in the spatial integration of motion signals. Spat Vis 12:287–307.

Dupont P, de Bruyn B, Vandenberghe R, Rosier A-M, Michiels J, Marchal G, Mortelmans L, Orban GA (1997): The kinetic occipital region in human visual cortex. Cereb Cortex 7:283–292.

Frässle S, Sommer J, Jansen A, Naber M, Einhauser W (2014): Binocular rivalry: Frontal activity relates to introspection and action but not to perception. J Neurosci 34:1738–1747.

Freeman E, Driver J (2008): Voluntary control of long-range motion integration via selective attention to context. J Vis 8: 1–22.

Friston KJ (2011): Functional and effective connectivity: A review. Brain Connect 1:13–36.

Friston KJ, Jezzard P, Turner R (1994): Analysis of functional MRI time-series. Hum Brain Mapp 1:

Friston KJ, Moran R, Seth AK (2013): Analysing connectivity with Granger causality and dynamic causal modelling. Curr Opin Neurobiol 23:172–178.

Genç E, Bergmann J, Singer W, Kohler A (2011): Interhemispheric connections shape subjective experience of bistable motion. Curr Biol 21:1494–1499.

Genç E, Schölvinck ML, Bergmann J, Singer W, Kohler A (2016): Functional connectivity patterns of visual cortex reflect its anatomical organization. Cereb Cortex 26:3719–3731.

Glover GH (1999): Deconvolution of impulse response in event-related BOLD fMRI. Neuroimage 9:416–429.

Goebel R, Roebroeck A, Kim D, Formisano E (2003): Investigating directed cortical interactions in time-resolved fMRI data using vector autoregressive modeling and Granger causality mapping. Magn Reson Imag 21:1251–1261.

de Graaf TA, de Jong MC, Goebel R, van Ee R, Sack AT (2011): On the functional relevance of frontal cortex for passive and voluntarily controlled bistable vision. Cereb Cortex 21: 2322–2331.

Guo K, Robertson RG, Pulgarin M, Nevado A, Panzeri S, Thiele A, Young MP (2007): Spatio-temporal prediction and inference by V1 neurons. Eur J Neurosci 26:1045–1054.

Huk AC, Dougherty RF, Heeger DJ (2002): Retinotopy and functional subdivision of human areas MT and MST. J Neurosci 22: 7195–7205.

Huk AC, Heeger DJ (2002): Pattern-motion responses in human visual cortex. Nat Neurosci 5:72–75.

Intaitė M, Duarte JV, Castelo-Branco M (2016): Working memory load influences perceptual ambiguity by competing for fronto-parietal attentional resources. Brain Res 1650:142–151.

Intaitė M, Koivisto M, Castelo-Branco M (2014): The linear impact of concurrent working memory load on dynamics of Necker cube perceptual reversals. J Vis 14:

Kaas A, Weigelt S, Roebroeck A, Kohler A, Muckli L (2010): Imagery of a moving object: The role of occipital cortex and human MT/V5+. Neuroimage 49:794–804.

Kanai R, Bahrami B, Rees G (2010): Human parietal cortex structure predicts individual differences in perceptual rivalry. Curr Biol 20:1626–1630.

Kanai R, Carmel D, Bahrami B, Rees G (2011): Structural and functional fractionation of right superior parietal cortex in bistable perception. Curr Biol 21:R106–R107.

Kaneoke Y, Urakawa T, Hirai M, Kakigi R, Murakami I (2009): Neural basis of stable perception of an ambiguous apparent motion stimulus. Neuroscience 159:150–160.

van Kemenade BM, Seymour K, Christophel TB, Rothkirch M, Sterzer P (2014): Decoding pattern motion information in V1. Cortex 57:177–187.

Kleinschmidt A, Büchel C, Zeki S, Frackowiak RS (1998): Human brain activity during spontaneously reversing perception of ambiguous figures. Proc R Soc London Part B Biol Sci 265: 2427–2433.

Kline KA, Holcombe AO, Eagleman DM (2004): Illusory motion reversal is caused by rivalry, not by perceptual snapshots of the visual field. Vision Res 44:2653–2658.

Knapen T, Brascamp J, Pearson J, van Ee R, Blake R (2011): The role of frontal and parietal brain areas in bistable perception. J Neurosci 31:10293–10301.

Kolster H, Peeters R, Orban GA (2010): The retinotopic organization of the human middle temporal area MT/V5 and its cortical neighbors. J Neurosci 30:9801–9820.

Kozak LR, Castelo-Branco M (2009): Peripheral influences on motion integration in foveal vision are modulated by central local ambiguity and center-surround congruence. Investig Ophthalmol Vis Sci 50:980–988.

Kriegeskorte N, Goebel R (2001): An efficient algorithm for topologically correct segmentation of the cortical sheet in anatomical MR volumes. Neuroimage 14:329–346.

Lamichhane B, Adhikari BM, Dhamala M (2016): The activity in the anterior insulae is modulated by perceptual decision-making difficulty. Neuroscience 327:79–94.

Lamichhane B, Dhamala M (2015): Perceptual decision-making difficulty modulates feedforward effective connectivity to the dorsolateral prefrontal cortex. Front Hum Neurosci 9:1–9:

Leopold DA, Logothetis NK (1999): Multistable phenomena: Changing views in perception. Trends Cogn Sci 3:254–264.

Leopold DA, Wilke M, Maier A, Logothetis NK (2002): Stable perception of visually ambiguous patterns. Nat Neurosci 5:605–609.

Linden DE, Prvulovic D, Formisano E, Vollinger M, Zanella FE, Goebel R, Dierks T (1999): The functional neuroanatomy of target detection: An fMRI study of visual and auditory oddball tasks. Cereb Cortex 9:815–823.

Liu T, Slotnick SD, Yantis S (2004): Human MT+ mediates perceptual filling-in during apparent motion. Neuroimage 21:1772–1780.

Liu Z, Zhang N, Chen W (2009): Mapping the bilateral visual integration by EEG and fMRI. Neuroimage 46:989–997.

Long GM, Toppino TC (2004): Enduring interest in perceptual ambiguity: Alternating views of reversible figures. Psychol Bull 130:748–768.

Lumer ED, Friston KJ, Rees G (1998): Neural correlates of perceptual rivalry in the human brain. Science 280:1930–1934.

Lumer ED, Rees G (1999): Covariation of activity in visual and prefrontal cortex associated with subjective visual perception. Proc Natl Acad Sci USA 96:1669–1673.

McDermott J, Weiss Y, Adelson EH (2001): Beyond junctions: Nonlocal form constraints on motion interpretation. Perception 30:905–921.

Megumi F, Bahrami B, Kanai R, Rees G (2015): Brain activity dynamics in parietal regions during spontaneous switch in bistable perception. Neuroimage 107:190–197.

Movshon JA, Newsome WT (1996): Visual response properties of striate cortical neurons projecting to area MT in macaque monkeys. J Neurosci 16:7733–7741.

Muckli L, Kohler A, Kriegeskorte N, Singer W (2005): Primary visual cortex activity along the apparent-motion trace reflects illusory perception. PLoS Biol 3:

Muckli L, Kriegeskorte N, Lanfermann H, Zanella FE, Singer W, Goebel R (2002): Apparent motion: Event-related functional magnetic resonance imaging of perceptual switches and states. J Neurosci 22:RC219.

Naghavi HR, Nyberg L (2005): Common fronto-parietal activity in attention, memory, and consciousness: Shared demands on integration?. Conscious Cogn 14:390–425.

O'Craven KM, Rosen BR, Kwong KK, Treisman A, Savoy RL (1997): Voluntary attention modulates fMRI activity in human MT-MST. Neuron 18:591–598.

Oldfield R (1971): The assessment and analysis of handedness: The Edinburgh inventory. Neuropsychologia 9:97–113.

Van Oostende S, Sunaert S, Hecke P, Van, Marchal G, Orban GA (1997): The Kinetic Occipital (KO) region in man: An fMRI study. Cereb Cortex 7:690–701.

Pack CC, Livingstone MS, Duffy KR, Born RT (2003): End-stopping and the aperture problem: Two-dimensional motion signals in macaque V1. Neuron 39:671–680.

Pelli DG (1997): The VideoToolbox software for visual psychophysics: Transforming numbers into movies. Spat Vis 10: 437–442.

Penny W, Holmes A, Friston KJ (2003): Random effects analysis. In: Richard S, Frackowiak J, Friston KJ, Frith CD, Dolan R, Price CJ, Zeki S, Ashburner J, Penny W, editors. Human Brain Function. London: Academic Press.

Rebola J, Castelhano J, Ferreira C, Castelo-Branco M (2012): Functional parcellation of the operculo-insular cortex in perceptual decision making: An fMRI study. Neuropsychologia 50:3693–3701.

Reddy L, Rémy F, Vayssière N, VanRullen R (2011): Neural correlates of the continuous Wagon Wheel Illusion: A functional MRI study. Hum Brain Mapp 32:163–170.

Roebroeck A, Formisano E, Goebel R (2005): Mapping directed influence over the brain using Granger causality and fMRI. Neuroimage 25:230–242.

Roebroeck A, Formisano E, Goebel R (2011): The identification of interacting networks in the brain using fMRI: Model selection, causality and deconvolution. Neuroimage 58:296–302.

Rose M, Büchel C (2005): Neural coupling binds visual tokens to moving stimuli. J Neurosci 25:10101–10104.

Schmidt KE, Castelo-Branco M, Goebel R, Payne BR, Lomber SG, Galuske RA (2006): Pattern motion selectivity in population responses of area 18. Eur J Neurosci 24:2363–2374.

Schwarzkopf DS, Sterzer P, Rees G (2011): Decoding of coherent but not incoherent motion signals in early dorsal visual cortex. Neuroimage 15:688–698.

Serences JT, Boynton GM (2007): The representation of behavioral choice for motion in human visual cortex. J Neurosci 27: 12893–12899.

Seth AK, Barrett AB, Barnett L (2015): Granger causality analysis in neuroscience and neuroimaging. J Neurosci 35:3293–3297.

Seth AK, Chorley P, Barnett LC (2013): Granger causality analysis of fMRI BOLD signals is invariant to hemodynamic convolution but not downsampling. Neuroimage 65:540–555.

Shimono M, Mano H, Niki K (2012): The brain structural hub of interhemispheric information integration for visual motion perception. Cereb Cortex 22:337–344.

Simoncelli EP, Heeger DJ (1998): A model of neuronal responses in visual area MT. Vision Res 38:743–761.

Stephan KE, Friston KJ (2010): Analyzing effective connectivity with fMRI. Wiley Interdiscip Rev Cogn Sci 1:446–459.

Sterzer P, Haynes J-D, Rees G (2006): Primary visual cortex activation on the path of apparent motion is mediated by feedback from hMT+/V5. Neuroimage 32:1308–1316.

Sterzer P, Kleinschmidt A (2007): A neural basis for inference in perceptual ambiguity. Proc Natl Acad Sci USA 104:323–328.

Sterzer P, Russ MO, Preibisch C, Kleinschmidt A (2002): Neural correlates of spontaneous direction reversals in ambiguous apparent visual motion. Neuroimage 15:908–916.

Stottinger E, Filipowicz A, Valadao D, Culham JC, Goodale MA, Anderson B, Danckert J (2015): A cortical network that marks the moment when conscious representations are updated. Neuropsychologia 79:113–122.

Tinsley CJ, Webb BS, Barraclough NE, Vincent CJ, Parker A, Derrington AM (2003): The nature of V1 neural responses to 2D moving patterns depends on receptive-field structure in the marmoset monkey. J Neurophysiol 90:930–937.

Tootell RB, Mendola JD, Hadjikhani NK, Ledden PJ, Liu AK, Reppas JB, Sereno MI, Dale AM (1997): Functional analysis of V3A and related areas in human visual cortex. J Neurosci 17:7060–7078.

Tsuchiya N, Wilke M, Frassle S, Lamme VA (2015): No-report paradigms: Extracting the true neural correlates of consciousness. Trends Cogn Sci 19:757–770.

Wallach H (1935): Über visuell wahrgenommene Bewegungsrichtung. Psychol Forsch 20:325–380.

Weilnhammer VA, Ludwig K, Hesselmann G, Sterzer P (2013): Frontoparietal cortex mediates perceptual transitions in bistable perception. J Neurosci 33:16009–16015.

Wenderoth P, Alais D, Burke D, van der Zwan R (1994): The role of the blobs in determining the perception of drifting plaids and their motion aftereffects. Perception 23:1163–1169.

Wernery J (2013): Bistable Perception of the Necker Cube in the Context of Cognition & Personality.

Wibral M, Bledowski C, Kohler A, Singer W, Muckli L (2009): The timing of feedback to early visual cortex in the perception of long-range apparent motion. Cereb Cortex 19:1567–1582.

Wuerger S, Shapley R, Rubin N (1996): "On the visually perceived direction of motion" by Hans Wallach: 60 years later. Perception 25:1317–1367.

Zaretskaya N, Thielscher A, Logothetis NK, Bartels A (2010): Disrupting parietal function prolongs dominance durations in binocular rivalry. Curr Biol 20:2106–2111.

Zeki S, Watson J, Lueck C, Friston KJ, Kennard C, Frackowiak RS (1991): A direct demonstration of functional specialization in human visual cortex. J Neurosci 11:641–649.

Zhou Y, Gao J, White K, Merk I, Yao K (2004): Perceptual dominance time distributions in multistable visual perception. Biol Cybern 90:256–263.